

Accepted Manuscript

Endoplasmic reticulum-targeted two-photon turn-on fluorescent probe for nitroreductase in tumor cells and tissues

An Xu, Yonghe Tang, Weiyang Lin



PII: S1386-1425(18)30493-1
DOI: [doi:10.1016/j.saa.2018.05.092](https://doi.org/10.1016/j.saa.2018.05.092)
Reference: SAA 16126

To appear in: *Spectrochimica Acta Part A: Molecular and Biomolecular Spectroscopy*

Received date: 1 March 2018
Revised date: 18 May 2018
Accepted date: 27 May 2018

Please cite this article as: An Xu, Yonghe Tang, Weiyang Lin , Endoplasmic reticulum-targeted two-photon turn-on fluorescent probe for nitroreductase in tumor cells and tissues. *Spectrochimica Acta Part A: Molecular and Biomolecular Spectroscopy*(2017), doi:[10.1016/j.saa.2018.05.092](https://doi.org/10.1016/j.saa.2018.05.092)

This is a PDF file of an unedited manuscript that has been accepted for publication. As a service to our customers we are providing this early version of the manuscript. The manuscript will undergo copyediting, typesetting, and review of the resulting proof before it is published in its final form. Please note that during the production process errors may be discovered which could affect the content, and all legal disclaimers that apply to the journal pertain.

Endoplasmic reticulum-targeted two-photon turn-on
fluorescent probe for nitroreductase in tumor cells and
tissues

An Xu, Yonghe Tang, Weiying Lin*

Institute of Fluorescent Probes for Biological Imaging, School of Chemistry and
Chemical Engineering, School of Materials Science and Engineering, University of
Jinan, Jinan, Shandong 250022, P.R. China.

*Corresponding author. Tel.: +86 53182769108; Fax: +86-531-82769031

E-mail address: weiylinglin2013@163.com.

Abstract

Hypoxia conditions could increase the activity of intracellular nitroreductase (NTR) and lead to many malignant diseases. Therefore, monitoring the activity of NTR is of great significance to study the related diseases. Organelles play crucial roles in the metabolism of living cells. In these organelles, the endoplasmic reticulum (ER) possesses single membrane structure, and it is the largest organelle in the cell. ER performs the synthesis, processing and modification of proteins and lipid, stabilizing the intracellular Ca^{2+} concentration and other physiological functions in living cells. Therefore, it is of great significance to develop ER-target probes in living system. Toward this goal, a new endoplasmic reticulum-targeted two-photon fluorescence turn-on NTR probe **Na-NTR-ER** is designed and synthesized. Probe **Na-NTR-ER** has been proved to display high sensitivity (36 ng/mL) and selectivity to NTR. Particularly, probe **Na-NTR-ER** has been successfully applied for the monitoring of NTR in ER with a high the Pearson's colocalization coefficient as 0.90 in HeLa cells and cancerous mouse tissues up to the depth of 100 μm with significant fluorescence signals.

Key Words: Fluorescence Probe; Two-photon Excited Fluorescence; Endoplasmic Reticulum; Nitroreductase; Fluorescence Imaging

1. Introduction

Hypoxia could lead to many malignant diseases [1-5]. Recent researches have shown that cells under hypoxia conditions may produce elevated levels of specific bioreductase, such as nitroreductase (NTR), azoreductase, quinone reductase, and DT-diaphorase [6-10]. Amongst, NTRs belong to a kind of flavin-containing enzymes [11], which can reduce the nitro group to the corresponding amino moiety with the help of nicotinamide adenine dinucleotide (NADH) through a series of one-electron reduction processes [12]. In recent years, NTRs, as prodrug-activating enzyme, are also used for cancer gene therapy [13-15]. Therefore, it is of great significance to monitor the bioactivity of NTR in living system.

Most eukaryotic cells contain certain organelles, such as endoplasmic reticulum (ER), mitochondria, lysosomes, and Golgi apparatus. In these organelles, the ER is the largest organelle in the cell with single membrane structure, which plays a significant role in living systems and involves a great deal of essential biological processes [16], including synthesis, processing and modification of proteins and lipid, maintaining the intracellular Ca^{2+} concentration, and so on [17]. Furthermore, ER is also closely related to other organelles in living cells [18-20]. On the other hand, the hypoxia condition may affect ER homeostasis and causing an imbalance between protein folding load and capacity, which is known as 'ER stress', and this cellular process is frequently found in tumor cells [21-22]. Therefore, it is very important to develop a ER-targeted NTR fluorescent probe for further disentangling physiopathological function of ER.

Fluorescence imaging technique has received wide attention because of its high sensitivity and selectivity, fast response, and technical simplicity [23-25]. Particularly, the two-photon (TP) fluorescence imaging shows many advantages, such as higher spatial resolution, deep penetration, and low background fluorescence [26-29]. In recent years, several fluorescence probes have been reported to detect NTR [30-42]. However, the organelle-targeted two-photon fluorescent NTR probes are still lacking. In particular, there is no endoplasmic reticulum-targeted NTR fluorescent probe.

Therefore, the development of organelle-targeted (especially endoplasmic reticulum-targeted) two-photon NTR fluorescence probes has important value.

In this work, we reported a novel two-photon fluorescent probe **Na-NTR-ER** for detection of ER NTR in a turn-on mode. **Na-NTR-ER** was able to preferentially locate in the ER of the cells due to the methyl sulphonamide moiety [43-45]. Meanwhile, the probe showed good selectivity and sensitivity for NTR and was suitable for the detection of ER NTR in living HeLa cells by two-photon fluorescence microscope and confocal microscope. Significantly, we have successfully used the new probe to monitor ER NTR in both living cells and live tumor tissues of mice.

2. Experimental

2.1. Materials and instrumentation

Unless otherwise stated, all solvents and reagents were commercially available and used without further purification. Solvents used were purified by standard methods prior to use. Doubly distilled water was used throughout all experiments. Thin-layer chromatography (TLC) analysis was performed on silica gel plates and column chromatography was conducted over silica gel (mesh 200-300), both of which were obtained from the *Qingdao Ocean Chemicals*. MTT (3-(4,5-Dimethylthiazol-2-yl)-2,5-diphenyltetrazolium bromide) and Escherichia coli nitroreductase (NTR) were from *Sigma-Aldrich*. The NTR was dissolved into ultrapure water, and the enzyme solution was stored immediately at -80 °C to keep the enzyme activity, and thawed quickly at 37 °C before use. β -Nicotinamide adenine dinucleotide disodium salt (NADH) was purchased from *J&K Scientific Ltd*. ER-Tracker Red was purchased from *Beyotime Biotechnology co. Ltd*. High-resolution mass spectra (HRMS) were recorded on a Bruker Apex Ultra 7.0 T FTMS mass spectrometer in electrospray ionization (ESI) mode. The ^1H NMR and ^{13}C NMR spectra were recorded on a Bruker AVANCE III 400 MHz Digital NMR Spectrometer, and using DMSO- d_6 as solvent and tetramethylsilane (TMS) as internal reference respectively. UV-vis absorption spectra were recorded on a Shimadzu

UV-2600 UV-vis spectrophotometer and fluorescent spectra were measured on a Hitachi F-4600 luminescence spectrophotometer with a 1 cm standard quartz cell. The fluorescence imaging of cells was performed using a Nikon A1MP confocal microscope. The pH measurements were carried out on a Mettler-Toledo Delta 320 pH meter.

2.2. Synthesis of *Na-NTR-ER*

The synthetic routes of the probe **Na-NTR-ER** and compound **Na-ER** were shown in Scheme S1. Compound **2**, compound **7**, compound **8**, and compound **Na-ER** were synthesized according to the previous literature [43]. Compound **4** and compound **5** were also synthesized according to the previous reports [46].

Compound **2** (320 mg, 1.5 mmol) and compound **5** (243 mg, 1 mmol) were added to ethanol (20 mL), triethylamine (0.1 mL) was dropwise added to the above suspension with stirring at room temperature. After refluxing overnight, the reaction was cooled down to room temperature. The solvent was removed by evaporation under reduced pressure, and the resulting residue was further purified by column chromatography to obtain a brown yellow solid product **Na-NTR-ER** 224 mg with a yield of 51%. ^1H NMR (400 MHz, DMSO- d_6) δ 8.71 (dd, $J_1=8.7$ Hz, $J_2=0.9$ Hz, 1H), 8.60 (dd, $J_1=7.2$ Hz, $J_2=0.8$ Hz, 1H), 8.56 (m, 2H), 8.09 (td, $J_1=7.6$ Hz, $J_2=1.3$ Hz, 1H), 7.80 (t, $J=5.8$ Hz, 1H), 7.57 (d, $J=8.2$ Hz, 2H), 7.22 (d, $J=8.2$ Hz, 2H), 4.11 (t, $J=6.4$ Hz, 2H), 3.11 (q, $J=6.4$ Hz, 2H), 2.25 (s, 3H); ^{13}C NMR (100 MHz, DMSO- d_6) δ 163.48, 162.69, 149.60, 142.92, 138.16, 132.09, 130.55, 129.95, 129.17, 128.84, 127.12, 126.77, 124.65, 123.27, 123.14, 40.11, 21.30; HR-MS calculated for $\text{C}_{21}\text{H}_{17}\text{N}_3\text{O}_6\text{S}$ $[\text{M}+\text{H}]^+ m/z$ 440.0911, found 440.0913.

2.3. Spectrum measurement

All the spectrum measurements were carried out as following. The stock solution of **Na-NTR-ER** was prepared with the concentration of 1.0 mM in DMSO. NADH

was dissolved in ultrapure water to obtain the stock solution with a concentration of 100 mM. The other analytes were dissolved in ultrapure water to obtain appropriate concentration. For the spectrum test, the probe **Na-NTR-ER** (5.0 μM) and NADH (500 μM) were dissolved in 10 mM PBS buffer (pH 7.4, with 5 % DMSO as co-solvent). Before recording the spectra, the test solution was incubated with appropriate testing species for 60 min at 37 °C. The excitation wavelength of test solution was 440 nm. The test solution was shaken well and incubated with certain analytes for 60 min before recording the spectra.

2.4. MTT assays

The HeLa cells were cultured in Dulbecco's Modified Eagle Medium media (DMEM, Hyclone) supplemented with 10 % heat-inactivated fetal bovine serum (FBS, Sijiqing) in an atmosphere of 5% CO₂ and 95% air at 37 °C up to appropriate density. Before the experiments, the HeLa cells (1×10^4 /well) were placed in a 96-well plate and further cultured for another 24 h. Then the cells were incubated with varying concentrations of **Na-NTR-ER** (0, 1.0, 2.0, 5.0, 10.0 μM) at 37 °C for 24 h, followed by the MTT assays. Untreated groups were also conducted under the same conditions.

2.5. HeLa cells culture and hypoxic imaging in HeLa cells

The HeLa cells were inoculated into 35 mm glass-bottom culture dishes (Nest). The cells were incubated under the normoxic condition (21 % O₂) and the different hypoxic conditions (15-1 % O₂) for 12 h. The cells were added the probe **Na-NTR-ER** (5.0 μM) and further incubated under the same conditions for another 60 min at 37 °C, and then the HeLa cells were imaged with a two-photon (TP) fluorescence confocal microscope. The cells were excited with 488/760 nm (one-photon (OP)/two-photon (TP) mode), and the emission wavelengths were collected from 500 nm to 550 nm.

The co-localization experiment: the HeLa cells were incubated under the hypoxic conditions (1 % O₂) for 12 h, then added the probe **Na-NTR-ER** (5.0 μM), and further incubated under the same condition for another 60 min. After removing the

culture medium and washing the cells with PBS for three times, the cells were added the ER-Tracker Red (1.0 μM) and incubation for another 15 min.

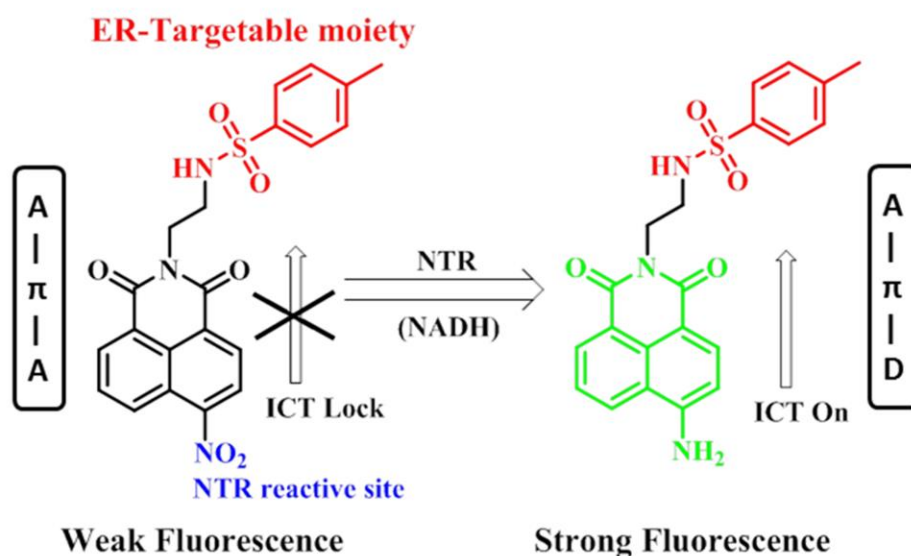
2.6. Rat tissue slices preparation and fluorescent imaging

Four weeks old Balb/c mice were kindly kept during the experiments. 4T-1 cells were injected to the mice. When the tumor grows to certain size, the mice were killed. Then the tumor tissues were removed from the mouse. After washing off the blood with PBS, the tumor tissues were cut into suitable size. After incubated with the probe **Na-NTR-ER** (30 μM) for 60 min, the tumor tissues were washed three times with PBS. Then the tumor tissue slices were imaged with a TP fluorescence microscope. The tissues were excited at 760 nm (TP mode), and the emission wavelengths were collected from 500 nm to 550 nm.

3. Results and discussion

3.1. Design and synthesis of Na-NTR-ER

The naphthylamide dye has outstanding TP fluorescent properties and is widely used in preparing various fluorescent probes [43, 47, 48]. The nitroaromatics are frequently used during the development of pro-drugs for hypoxia [6, 49, 50]. Consequently, we used naphthylamide as the fluorescent platform and nitro group as the NTR identification site, and introduced methyl sulphonamide moiety, the ER-target group, to construct a fluorescent NTR probe **Na-NTR-ER**. Due to the strong electron-withdrawing effect of the nitro group, the electron structure of the probe **Na-NTR-ER** behaved as “A- π -A”. The fluorescent probe had almost no fluorescence due to the specific electronic structure. Under the catalytic reduction of NTR, the nitro group was reduced to hydroxylamine, and then to amino moiety via a one-electron reduction pathway. The nitro moiety was eventually reduced to amine moiety, the strong electron-donating group, changes the electron structure of fluorophore from “A- π -A” to “D- π -A”. Consequently, the intramolecular charge transfer (ICT) effect of the molecule resulted in strong fluorescence of **Na-ER** (Scheme 1 and Scheme S2).



Scheme 1. The structures of the probe **Na-NTR-ER** and compound **Na-ER**, and the proposed recognition mechanism of the probe **Na-NTR-ER** for NTR.

3.2. Photophysical properties of *Na-NTR-ER*

After the fluorescence probe **Na-NTR-ER** was obtained, we first tested the absorption spectra in PBS buffer. As shown in the Fig. S1, the maximum absorption wavelength of **Na-NTR-ER** was about 356 nm ($\epsilon=19,200 \text{ M}^{-1} \text{ cm}^{-1}$). In contrast, the maximum absorption wavelength of **Na-ER** was about 440 nm ($\epsilon=19,600 \text{ M}^{-1} \text{ cm}^{-1}$). Similar to the absorption spectrum, the emission spectrum also had a significant change. As designed, due to the specific electronic structures of “A- π -A”, **Na-NTR-ER** showed almost non-fluorescent. Under the catalytic reduction of NTR, the nitro group was eventually reduced to amine group, an intense fluorescence peak around 543 nm was observed (Fig. 1). According to titration test, the detection limit of **Na-NTR-ER** for NTR was calculated as 36 ng/mL (Fig. S2). These data indicated that **Na-NTR-ER** has a high sensitivity to detect NTR, and the sensitivity of the already described methods could detect the NTR values reported for living systems.

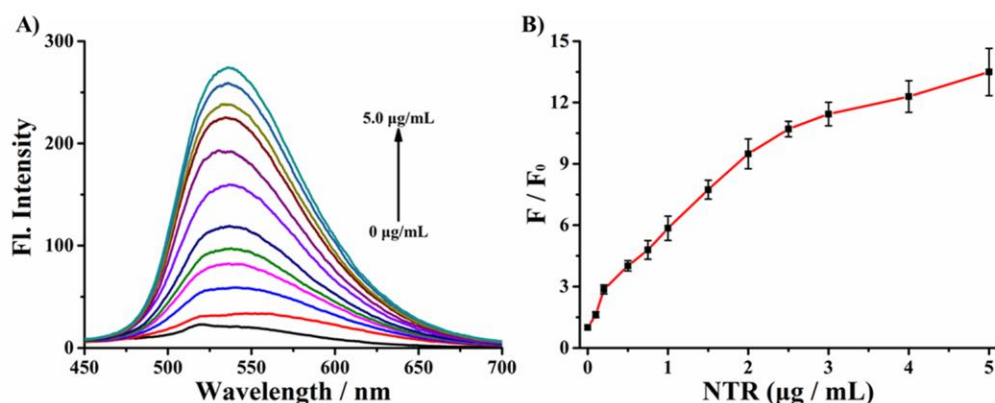


Fig. 1. (A) Fluorescence spectra of the probe **Na-NTR-ER** (5.0 μM) in 10 mM PBS buffer (pH 7.4, 5 % DMSO) with various concentrations of NTR (0-5.0 $\mu\text{g/mL}$) and NADH (500 μM) for 60 min at 37 $^{\circ}\text{C}$. (B) Fluorescence intensity ratio (F/F_0) changes at 543 nm of **Na-NTR-ER** (5.0 μM) with the amount of NTR (0-5.0 $\mu\text{g/mL}$) in the presence of NADH (500 μM). $\lambda_{\text{ex}} = 440$ nm. $n = 3$, $\text{RSD} \leq 10.2\%$ (B).

The response rate is also one of the basic parameters to evaluate the identification ability of the probe. The dynamic tests of the probe **Na-NTR-ER** (5.0 μM) treated with varying concentration of NTR (0-5.0 $\mu\text{g/mL}$) and NADH (500 μM) were carried out (Fig. S3). The fluorescent intensity of the probe (5.0 μM) only treated with NADH (500 μM) was almost unchanged. In comparison, after the probe incubated with NTR and NADH, strong changes of fluorescent signals were observed at about 543 nm. And the fluorescence signal could reach a plateau state after about 60 min. In spite of the response rate for NTR is not very fast, but the fluorescence enhancement ratio is enough to apply to cell imaging after 60 min.

The activity of biological enzymes is closely related to the change of temperature. We conducted experiment to investigate the fluorescent signal changes of **Na-NTR-ER** (5.0 μM) treated or untreated with NTR (2.0 $\mu\text{g/mL}$) and NADH (500 μM) at different temperatures (20-40 $^{\circ}\text{C}$). As shown in the Fig. S4, the fluorescence intensities of **Na-NTR-ER** had almost no change over a wide temperature range of 20-40 $^{\circ}\text{C}$ without NTR, suggesting that **Na-NTR-ER** is stable in this temperature

range. By contrast, after **Na-NTR-ER** was incubated with NTR (2.0 $\mu\text{g/mL}$) and NADH (500 μM) for 60 min, an intense fluorescence signal was observed. Especially under 37 $^{\circ}\text{C}$ (the physiological temperature condition), the fluorescence enhancement phenomenon was the most significant. Solution pH also has major influence on the activity of biological enzymes. The probe (5.0 μM) with NADH (500 μM) showed few fluorescence intensity changes in a wide pH range (from 4.0 to 10.0), while a remarkable fluorescent enhancement was observed when the NTR (2.0 $\mu\text{g/mL}$) was introduced especially at pH 7.4 (the physiological) (Fig. S5). These results reveal that **Na-NTR-ER** gives intense signals under about pH 7.4 and 37 $^{\circ}\text{C}$ (the physiological conditions) and is suitable for biological applications, which should be ascribed to rigorous reaction conditions of biological enzyme.

High selectivity is one of the basic characteristics of fluorescent probes for applications in complex biological system. Therefore, the probe **Na-NTR-ER** was incubated with various biologically relevant analytes, including biothiols (Cys, Hcy, GSH), cations/anions (Ca^{2+} , Cu^{2+} , Fe^{2+} , Mg^{2+} , Zn^{2+} , K^{+} , Na^{+} , F^{-} , Cl^{-} , Br^{-} , I^{-} , SCN^{-} , NO_2^{-} , NO_3^{-} , OAc^{-} , HS^{-} , SO_4^{2-}), reactive oxygen species (ROS) (H_2O_2 , HClO , *tert*-butyl hydroperoxide (TBHP), $\bullet\text{OH}$), and NTR, in PBS buffer. As shown in the Fig. S6, in the absence of NADH, all the analytes almost had hardly change the fluorescence emission intensity of the probe, suggesting that These results indicated those relevant substance do not interfere with the fluorescence of probe directly and NADH plays a key role in the process of enzymatic reduction. At the same condition, with the introduction of NADH, the other analytes (except NTR) also did not change the fluorescence intensity of the probe. By contrast, a strong turn-on signal was observed after **Na-NTR-ER** treated with NTR for 1 h (Fig. 2). The selection test results indicated that **Na-NTR-ER** is highly selective for NTR over other tested analytes, indicating that the probe is favorable for investigation of NTR in biological systems.

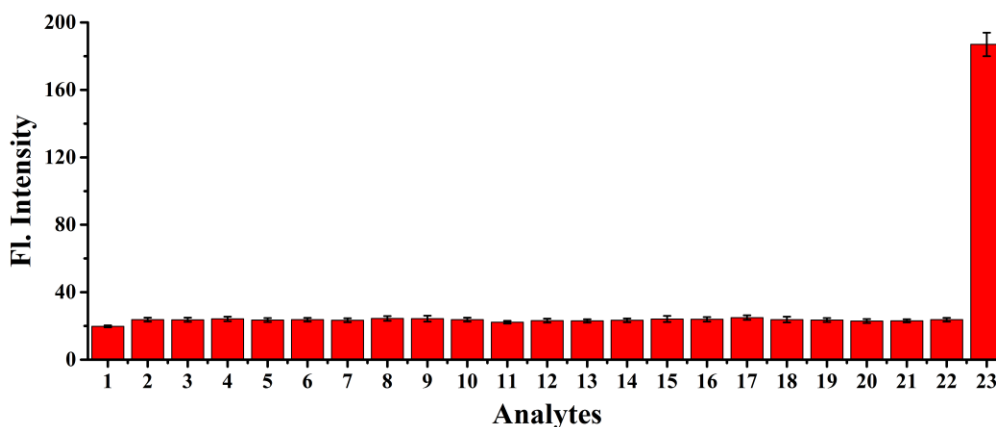


Fig. 2. Fluorescence responses of the probe **Na-NTR-ER** with various relevant analytes. The data were obtained after the incubation of the probe **Na-NTR-ER** (5.0 μM) with the analytes and NADH (500 μM) for 60 min at 37 $^{\circ}\text{C}$ in PBS buffer (pH 7.4, 5 % DMSO). Legend: (1) free probe; (2) CaCl_2 (2.5 mM); (3) CuCl_2 (2.5 mM); (4) FeSO_4 (2.5 mM); (5) MgCl_2 (100 μM); (6) ZnCl_2 (2.5 mM); (7) KF (2.5 mM); (8) KI (2.5 mM); (9) KSCN (2.5 mM); (10) NaBr (2.5 mM); (11) NaNO_2 (2.5 mM); (12) NaNO_3 (2.5 mM); (13) NaOAc (2.5 mM); (14) Na_2SO_4 (2.5 mM); (15) NaHS (2.5 mM); (16) Cys (2.5 mM); (17) GSH (2.5 mM); (18) Hcy (2.5 mM); (19) $\cdot\text{OH}$ (100 μM); (20) HClO (100 μM); (21) H_2O_2 (100 μM); (22) TBHP (100 μM); (23) NTR (2.0 $\mu\text{g/mL}$). $\lambda_{\text{ex}} = 440 \text{ nm}$. $n = 3$, $\text{RSD} \leq 7.5 \%$.

Moreover, the photostability of the probe was also tested. The irradiation of short wavelength (365 nm) UV-light did not change the fluorescence intensity of **Na-NTR-ER** (Fig. S7), suggesting that **Na-NTR-ER** has high photo-stability. We also used spectral experiments and HR-MS analyses to verify the identification mechanism of **Na-NTR-ER** for NTR. From the absorption spectrum, the maximum absorption wavelength of **Na-NTR-ER** was at about 356 nm. When NADH was introduced, a strong absorption peak was produced at 345 nm, which was the absorption peak of NADH, and the absorption peak was no change at about 440 nm. When NTR was added to the test solution, a new absorption peak had been generated at 440 nm, and the absorption peak is similar to that of compound **Na-ER** (Fig. S8). For the fluorescence emission spectra, when the probe treated with NTR and NADH,

a maximum fluorescence emission wavelength was found at 543 nm, which was also similar to the maximum emission wavelength of compound **Na-ER** (Fig. S9). The HR-MS analyses test result confirms that the reduction product of **Na-NTR-ER** and NTR is the compound **Na-ER**. (Fig. S10). These results agreed with the proposed mechanism in Scheme 1 and Scheme S2.

3.3. Fluorescence imaging of NTR in the living HeLa cells

As an imaging reagent, **Na-NTR-ER** should have low cytotoxicity. The data of cell cytotoxicity assay showed that the survival rate of HeLa cells remained above 90% (treated with 0-10 μM **Na-NTR-ER**) (Fig. S11), indicating that **Na-NTR-ER** has low cytotoxicity to the HeLa cells and **Na-NTR-ER** is suitable for imaging experiments.

Due to the activity of NTR is closely related to the degree of hypoxia in cells, we conducted NTR imaging experiments under different oxygen content conditions. As naphthylamide is a classic TP dye, we applied **Na-NTR-ER** for imaging NTR in the HeLa cells by the TP fluorescence and confocal microscope with the OP and TP modes. The HeLa cells displayed almost no fluorescent signal when the cell treated with **Na-NTR-ER** (5.0 μM) at normal oxygen content (21 % O_2) (Fig. 3A f, p). By contrast, when HeLa cells were cultured under hypoxic conditions (15–1% O_2) with **Na-NTR-ER** (5.0 μM), the different fluorescent signals were observed (Fig. 3A g-j and q-t). As the oxygen content decreases, the fluorescence intensity of the HeLa cells increased gradually (Fig. 3B and 3C). These studies demonstrated that **Na-NTR-ER** is suitable for monitoring the activity of endogenous NTR at different oxygen content in living HeLa cells by using OP/TP microscopical technique.

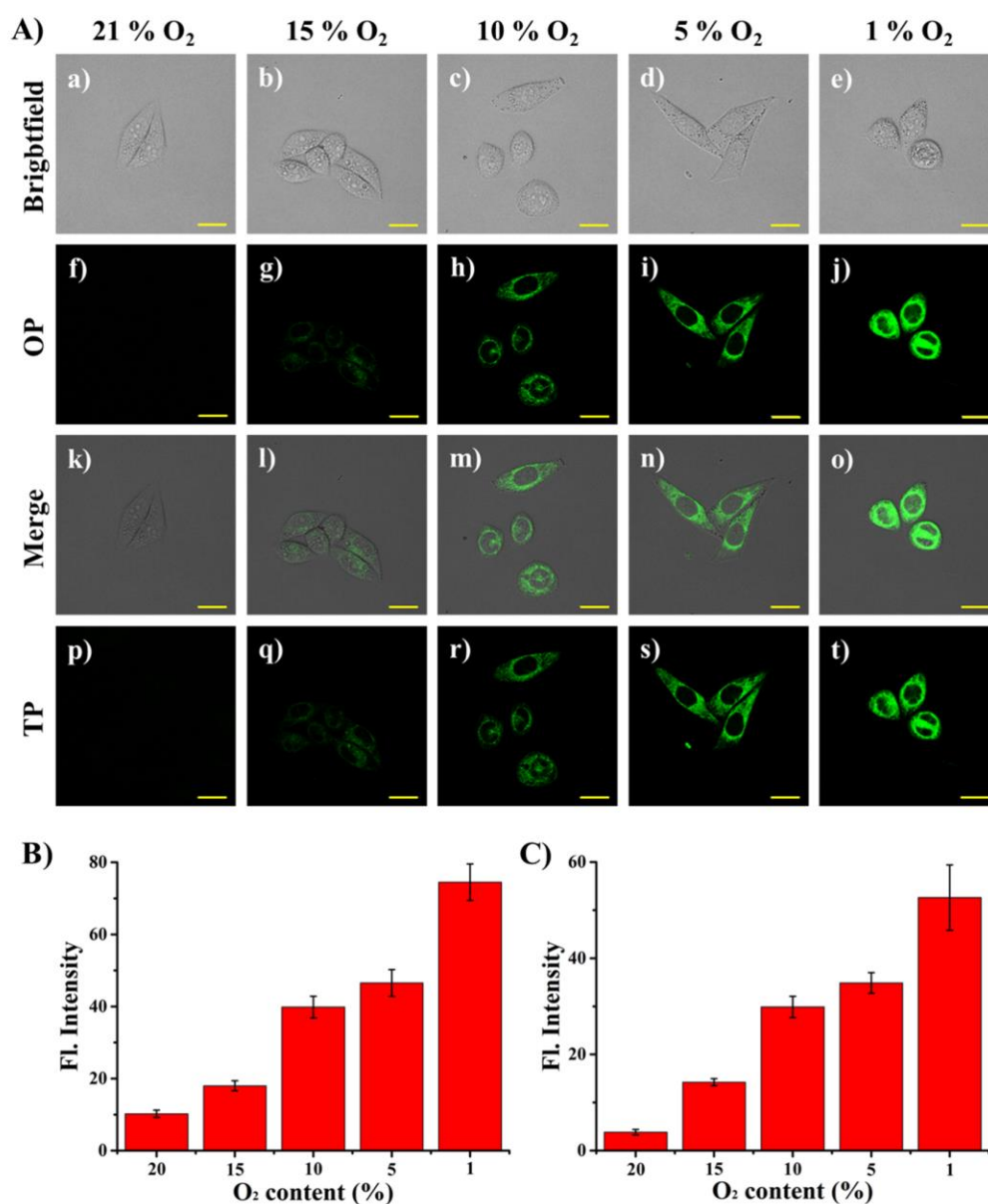


Fig. 3. A) Fluorescence imaging of NTR in the living HeLa cells. a-e) Bright-field image of the HeLa cells; f-j) One-photon image of HeLa cells; k-o) The merge of the bright-field image and one-photon image; p-t) Two-photon fluorescence images of the HeLa cells. Scale bar: 20 μ m. B) The one-photon fluorescence intensity of the HeLa cells images, $n=3$, $RSD \leq 9.8\%$. C) The two-photon fluorescence intensity of the HeLa cells images, $n=3$, $RSD \leq 14.6\%$.

3.4. Colocalization experiments of the probe in the living cells

We also conducted co-localization experiment to detect the targeted-feasibility of **Na-NTR-ER** in living cells. The HeLa cells were incubated with **Na-NTR-ER** and ER-Tracker Red (Beyotime Institute of Biotechnology) under hypoxic conditions (1% O₂). The HeLa cells showed significant green fluorescence as **Na-NTR-ER** reacted with the NTR (Fig. 4a). At the same time, strong red fluorescence was observed in the HeLa cells due to the presence of ER-Tracker Red (Fig. 4b). The merged image showed that the green fluorescence and the red fluorescence can be highly overlapped (Fig. 4c). Two fluorescence channels show high co-localization coefficients, the Pearson's colocalization coefficient was 0.90, and the Mander's overlap coefficient was 0.91 (Fig. 4d). In addition, the spatial distribution of the two fluorescent probes in HeLa cells also tended to be consistent (Fig. 4e). These results demonstrated that, as designed, **Na-NTR-ER** can be highly enriched in the ER of cells and can be used to imaging the NTR in the ER.

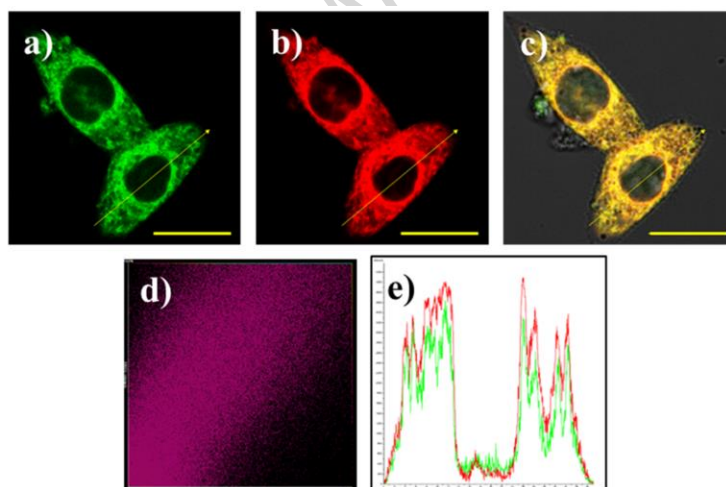


Fig. 4. The images of the living HeLa cells co-incubated with the probe **Na-NTR-ER** (5 μ M), and ER-TrackerTM Red under hypoxic condition (1% O₂). a) The fluorescence image of the green channel; b) The fluorescence image of the red channel; c) The merged image of a and b; d) Intensity scatter plot of the green and red channels. e) Intensity profile of linear region of interest across in the HeLa cells

co-stained with ER-Tracker Red and green channel of **Na-NTR-ER**. Scale bar: 20 μm .

3.5. Two-photon fluorescence imaging of NTR in living mouse tumor tissues

We also applied **Na-NTR-ER** to carry out the tissue imaging experiment to detect NTR in the living mouse tumor tissues by using TP fluorescence microscope. For a control experiment, the tumor tissue slides showed almost no fluorescence without the incubation of fluorescent probes (Fig. 5a). By contrast, the tumor tissue slides treated with **Na-NTR-ER** displayed green fluorescent emission up to a depth of 100 μm (Fig. 5b). The sharp experiment contrast demonstrated that **Na-NTR-ER** is suitable for monitoring the activity of endogenous NTR in living tissues by using TP microscopical technique.

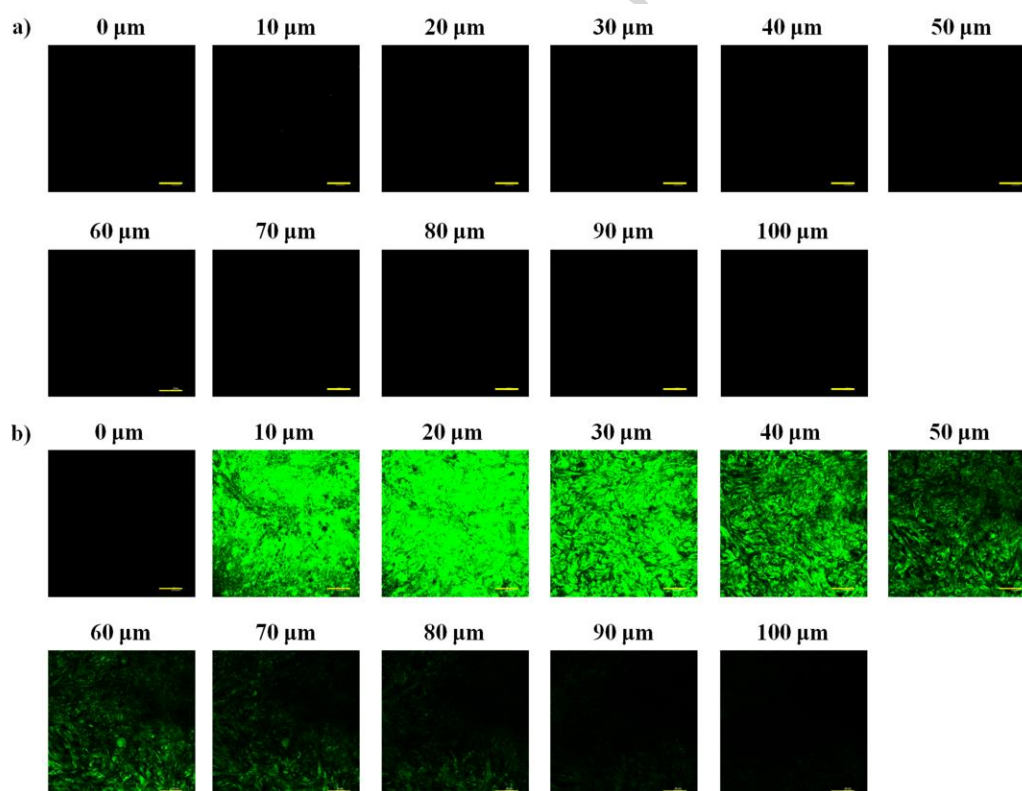


Fig. 5. Two-photon fluorescence imaging of NTR in the living tumor tissue slices. Fluorescence images of the tumor tissue slices incubated with the probe **Na-NTR-ER** (30 μM) for 60 min. Excitation was at 760 nm by femtosecond laser, and the emission

collection was from 500-550 nm. Scale bar: 20 μm .

4. Conclusions

In this work, we reported a novel two-photon fluorescent probe, **Na-NTR-ER** for the detection of ER NTR. **Na-NTR-ER** can be highly enriched in the ER of cells, and it is the first ER-targeted NTR fluorescent probe. The identification site, nitro group, is directly connected to the fluorescence platform 1,8-naphthalimide and causes the fluorescence quenching. After the catalytic reduction by NTR, a strong fluorescence signal was observed at 543 nm. Overall, **Na-NTR-ER** has several advantages in bioimaging experiments, such as high sensitivity and selectivity to NTR, low cytotoxicity, optimal responses in a physiological environment (physiological pH 7.4 and temperature 37 °C). Especially, **Na-NTR-ER** can be used to detect the activity of endogenous NTR at different oxygen content in living HeLa cells. **Na-NTR-ER** was successfully applied to detect endogenous NTR in the living mouse tumor tissues, and the penetration depth was up to 100 μm . Importantly, base on the excellent ER-targeted feature of **Na-NTR-ER**, we believe that **Na-NTR-ER** as a powerful molecular tool for studying the physiological function of NTR in ER of living cells and tissues.

Acknowledgements

This work was financially supported by NSFC (21472067, 21672083), Taishan Scholar Foundation (TS201511041), and the startup fund of University of Jinan (309-10004).

References

- [1] G.L. Semenza, Angiogenesis ischemic and neoplastic disorders, *Annu. Rev. Med.* 54 (2003) 17-28.
- [2] J.H. Crawford, T.S. Isbell, Z. Huang, S. Shiva, B.K. Chacko, A.N. Schechter, et

al., Hypoxia, red blood cells, and nitrite regulate NO-dependent hypoxic vasodilation, *Blood* 107 (2006) 566-574.

[3] C. Murdoch, M. Muthana, C.E. Lewis, Hypoxia regulates macrophage functions in inflammation, *J. Immunol.* 175 (2005) 6257-6263.

[4] S. Kizaka-Kondoh, M. Inoue, H. Harada, M. Hiraoka, Tumor hypoxia: a target for selective cancer therapy, *Cancer Sci.* 94 (2003) 1021-1028.

[5] A.L. Harris, Hypoxia--a key regulatory factor in tumour growth, *Nat. Rev. Cancer* 2 (2002) 38-47.

[6] J.M. Brown, W.R. Wilson, Exploiting tumour hypoxia in cancer treatment, *Nat. Rev. Cancer* 4 (2004) 437-447.

[7] T. Guo, L. Cui, J. Shen, W. Zhu, Y. Xu, X. Qian, A highly sensitive long-wavelength fluorescence probe for nitroreductase and hypoxia: selective detection and quantification, *Chem. Commun.* 49 (2013) 10820-10822.

[8] H. Komatsu, H. Harada, K. Tanabe, M. Hiraoka, S.i. Nishimoto, Indolequinone-rhodol conjugate as a fluorescent probe for hypoxic cells: enzymatic activation and fluorescence properties, *MedChemComm* 1 (2010) 50-53.

[9] R.J. Riley, P. Workman, DT-diaphorase and cancer chemotherapy, *Biochem. Pharmacol* 43 (1992) 1657-1669.

[10] M.I. Uddin, S.M. Evans, J.R. Craft, L.J. Marnett, M.J. Uddin, A. Jayagopal, Applications of azo-based probes for imaging retinal hypoxia, *ACS Med. Chem. Lett.* 6 (2015) 445-449.

[11] C.A. Haynes, R.L. Koder, A.F. Miller, D.W. Rodgers, Structures of nitroreductase in three states: effects of inhibitor binding and reduction, *J. Biol. Chem.* 277 (2002) 11513-11520.

[12] D.W. Bryant, D.R. McCalla, M. Leeksa, P. Laneuville, Type I nitroreductases of *escherichia coli*, *Can. J. Microbiol.* 27 (1981) 81-86.

[13] C. Berne, L. Betancor, H.R. Luckarift, J.C. Spain, Application of a microfluidic reactor for screening cancer prodrug activation using silica-immobilized nitrobenzene nitroreductase, *Biomacromolecules* 7 (2006) 2631-2636.

[14] J.I. Grove, A.L. Lovering, C. Guise, P.R. Race, C.J. Wrighton, S.A. White, et al.,

Generation of *escherichia coli* nitroreductase mutants conferring improved cell sensitization to the prodrug CB1954, *Cancer Res.* 63 (2003) 5532-5537.

[15] P.F. Searle, M.J. Chen, L. Hu, P.R. Race, A.L. Lovering, J.I. Grove, et al., Nitroreductase: a prodrug-activating enzyme for cancer gene therapy, *Clin. Exp. Pharmacol. Physiol.* 31 (2004) 811-816.

[16] P. Quinn, G. Griffiths, G. Warren, Density of newly synthesized plasma membrane proteins in intracellular membranes II. Biochemical studies, *J. Cell Biol.* 98 (1984) 2142-2147.

[17] O. Baumann, B. Walz, Endoplasmic reticulum of animal cells and its organization into structural and functional domains, *Int. Rev. Cytol.* 205 (2001) 149-214.

[18] D. Peretti, N. Dahan, E. Shimoni, K. Hirschberg, S. Lev, Coordinated lipid transfer between the endoplasmic reticulum and the golgi complex requires the VAP proteins and is essential for golgi-mediated transport, *Mol. Biol. Cell* 19 (2008) 3871-3884.

[19] H. Pichler, B. Gaigg, C. Hrastnik, G. Achleitner, S.D. Kohlwein, G. Zellnig, A. Perktold, et al., A subfraction of the yeast endoplasmic reticulum associates with the plasma membrane and has a high capacity to synthesize lipids, *Eur. J. Biochem.* 268 (2001) 2351-2561.

[20] J.R. Friedman, G.K. Voeltz, The ER in 3D: a multifunctional dynamic membrane network, *Trends Cell Biol.* 21 (2011) 709-717.

[21] A.H. Schonthal, Pharmacological targeting of endoplasmic reticulum stress signaling in cancer, *Biochem. Pharmacol.* 85(2013) 653-666.

[22] T. Verfaillie, A. D. Garg, P. Agostinis, Targeting ER stress induced apoptosis and inflammation in cancer, *Cancer Lett.* 332(2013) 249-264.

[23] J.R. Lakowicz (Eds.), Principles of fluorescence spectroscopy, Springer US, Boston, MA, 2006.

[24] X. Cao, W. Lin, and W. Wan. Development of a near-infrared fluorescent probe for imaging of endogenous Cu⁺ in live cells. *Chem. Commun.* 48 (2012) 6247 - 6249.

[25] S. Zhu, W. Lin, and L. Yuan. Development of a near-infrared fluorescent probe

for monitoring hydrazine in serum and living cells, *Anal. Methods* 5 (2013) 3450-3453.

[26] M. Göppert-Mayer, Über elementarakte mit zwei quantensprüngen, *Ann. Phys.* 401 (1931) 273-294.

[27] E. Bayer, G. Schaack, Two-photon absorption of $\text{CaF}_2:\text{Eu}^{2+}$, *Phys. Stat. Sol.* 41 (1970) 827-835.

[28] Y. Tang, X. Kong, A. Xu, B. Dong, W. Lin, Development of a two-photon fluorescent probe for imaging of endogenous formaldehyde in living tissues, *Angew. Chem. Int. Edit.* 55(2016) 3356-3359.

[29] B. Dong, X. Song, X. Kong, C. Wang, Y. Tang, Y. Liu, and W. Lin*. Simultaneous near-Infrared and two-photon in vivo imaging of H_2O_2 using a ratiometric fluorescent probe based on the unique oxidative rearrangement of oxonium, *Adv. Mater.* 28 (2016) 8755-8759.

[30] R.B.P. Elmes, Bioreductive fluorescent imaging agents: applications to tumour hypoxia, *Chem. Commun.* 52 (2016) 8935-8956.

[31] B.N. Lizama-Manibusan, S. Klein, J.R. McKenzie, D.E. Cliffe, B. McLaughlin, Analysis of a nitroreductase-based hypoxia sensor in primary neuronal cultures, *ACS Chem. Neurosci.* 7 (2016) 1188-1191.

[32] J. Zhou, W. Shi, L.H. Li, Q.Y. Gong, X.F. Wu, X.H. Li, et al., A lysosome-targeting fluorescence off-on probe for imaging of nitroreductase and hypoxia in live cells, *Chem. Asian J.* 11 (2016) 2719-2724.

[33] P. Feng, H. Zhang, Q. Deng, W. Liu, L. Yang, G. Li, et al., Real-time bioluminescence imaging of nitroreductase in mouse model, *Anal. Chem.* 88 (2016) 5610-5614.

[34] W. Feng, C. Gao, W. Liu, H. Ren, C. Wang, K. Ge, S. Li, G. Zhou, H. Li, S. Wang, G. Jia, Z. Li, J. Zhang, A novel anticancer theranostic pro-prodrug based on hypoxia and photo sequential control, *Chem. Commun.* 52 (2016) 9434-9437.

[35] A. Chevalier, Y. Zhang, O.M. Khmour, J.B. Kaye, S.M. Hecht, Mitochondrial nitroreductase activity enables selective imaging and therapeutic targeting, *J. Am. Chem. Soc.* 138 (2016) 12009-12012.

- [36] A. Xu, Y. Tang, Y. Ma, G. Xu, S. Gao, Y. Zhao, et al., A fast-responsive two-photon fluorescent turn-on probe for nitroreductase and its bioimaging application in living tissues, *Sens. Actuat. B: Chem* 252 (2017) 927-933.
- [37] S. Luo, Y. Liu, F. Wang, Q. Fei, B. Shi, J. An, C. Zhao, et al., A fluorescent turn-on probe for visualizing lysosomes in hypoxic tumor cells, *Analyst*, 141 (2016) 2879-2882.
- [38] D. Zhu, L. Xue, G. Li, H. Jiang, A highly sensitive near-infrared ratiometric fluorescent probe for detecting nitroreductase and cellular imaging, *Sens. Actuat. B: Chem* 222 (2016) 419-424.
- [39] X. Zhang, Q. Zhao, Y. Li, X. Duan, Y. Tang, Multifunctional probe based on cationic conjugated polymers for nitroreductase-related analysis: sensing, hypoxia diagnosis, and imaging, *Anal. Chem.* 89 (2017) 5503-5510.
- [40] D. Li, Y. Xu, N. Zhou, J. Liu, R. Wang, T. Cheng, et al., A novel “donor-two-acceptor” type fluorophore-based probe for fast detection and intracellular imaging of nitroreductase, *Dyes Pigm.* 136 (2017) 627-632.
- [41] A. Abuteen, F. Zhou, C. Dietz, I. Mohammad, M.B. Smith, Q. Zhu, Synthesis of a 4-nitroimidazole indocyanine dye-conjugate and imaging of tumor hypoxia in BALB/c tumor-bearing female mice, *Dyes Pigm.* 126 (2016) 251-260.
- [42] Y. Zhou, K.N. Bobba, X.W. Lv, D. Yang, N. Velusamy, J.F. Zhang, et al., Biotinylated piperazine-rhodol derivative: a ‘turn-on’ probe for nitroreductase triggered hypoxia imaging, *Analyst* 142 (2017) 345-350.
- [43] Y. Tang, A. Xu, Y. Ma, G. Xu, S. Gao, W. Lin, A turn-on endoplasmic reticulum-targeted two-photon fluorescent probe for hydrogen sulfide and bio-imaging applications in living cells, tissues, and zebrafish, *Sci. Rep.* 7 (2017) 12944-12952.
- [44] H. Xiao, P. Li, X. Hu, X. Shi, W. Zhang, B. Tang, Simultaneous fluorescence imaging of hydrogen peroxide in mitochondria and endoplasmic reticulum during apoptosis, *Chem. Sci.* 7 (2016) 6153-6159.
- [45] S. Xu, H.W. Liu, X.X. Hu, S.Y. Huan, J. Zhang, Y.C. Liu, L. Yuan, et al., Visualization of endoplasmic reticulum aminopeptidase 1 under different redox

conditions with a two-photon fluorescent probe, *Anal. Chem.* 89 (2017) 7641-7648.

[46] Y. Liu, D. Duan, J. Yao, B. Zhang, S. Peng, H. Ma, Y. Song, J. Fang, Dithiaarsanes induce oxidative stress-mediated apoptosis in HL-60 cells by selectively targeting thioredoxin reductase, *J. Med. Chem.* 57 (2014) 5203-5211.

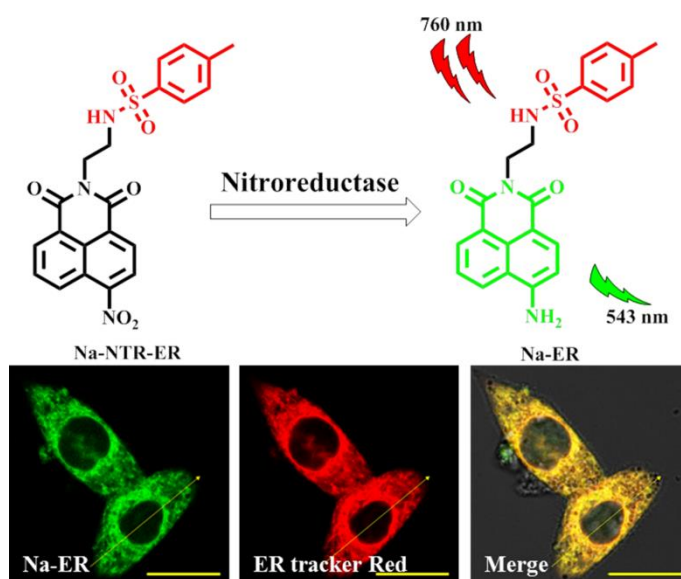
[47] H. Yu, Y. Xiao, L. Jin, A lysosome-targetable and two-photon fluorescent probe for monitoring endogenous and exogenous nitric oxide in living cells, *J. Am. Chem. Soc.* 134 (2012) 17486-17489.

[48] M. Ren, B. Deng, J.Y. Wang, X. Kong, Z.R. Liu, K. Zhou, L. He, W. Lin, A fast responsive two-photon fluorescent probe for imaging H₂O₂ in lysosomes with a large turn-on fluorescence signal, *Biosens. Bioelectron.* 79 (2016) 237-243.

[49] G. Xu, H.L. McLeod, Strategies for enzyme/prodrug cancer therapy, *Clin. Cancer Res.* 7 (2001) 3314-3324.

[50] W.A. Denny, The role of hypoxia-activated prodrugs in cancer therapy, *Lancet Oncol.* 1 (2000) 25-29.

Graphical Abstract



A new turn-on endoplasmic reticulum-targeted two-photon fluorescent probe (**Na-NTR-ER**) for nitroreductase was engineered for monitoring nitroreductase in the living cells and tissues.

Highlights

- 1) The probe **Na-NTR-ER** is a novel two-photon fluorescent nitroreductase (NTR) probe.
- 2) The probe **Na-NTR-ER** is the first fluorescent ER-targeted probe for NTR.
- 3) The probe **Na-NTR-ER** shows high selectivity and sensitivity to NTR.
- 4) The probe **Na-NTR-ER** could respond for the degree of hypoxia in the living cells.
- 5) The probe **Na-NTR-ER** could monitor NTR in tumor tissues up to depth of 100 μm .